archives
of thermodynamics
Vol. **34**(2013), No. 1, 55–69
DOI: 10.2478/aoter-2013-0004

Application of the finite element method to the determining of boiling heat transfer coefficient for minichannel flow

MAGDALENA PIASECKA[*1]
BEATA MACIEJEWSKA[2]

[1] Kielce University of Technology; Faculty of Mechatronics and Machine Building, Chair of Mechanics, al. 1000-lecia P.P.7, 25-314 Kielce, Poland

[2] Kielce University of Technology, Faculty of Management and Computer Modelling, Chair of Mathematics, al. 1000-lecia P.P.7, Kielce, 25-314 Poland

Abstract Miniature heat exchangers are used to provide higher cooling capacity for new technologies. This means a reduction in their size and cost but the identical power. The paper presents the method for determination of boiling heat transfer coefficient for a rectangular minichannel of 0.1 mm depth, 40 mm width and 360 mm length with asymmetric heating. Experimental research has focused on the transition from single phase forced convection to nucleate boiling, i.e., the zone of boiling incipience. The 'boiling front' location has been determined from the temperature distribution of the heated wall obtained from liquid crystal thermography. The experiment has been carried out with R-123, mass flux 220 kg/(m^{2}s), pressure at the channel inlet 340 kPa. Local values of heat transfer coefficient were calculated on the basis of empirical data from the experiment following the solution of the two-dimensional inverse heat transfer problem. This problem has been solved with the use of the finite element method in combination with Trefftz functions. Temperature approximates (linear combinations of Trefftz functions) strictly fulfill the governing equations. In presented method the inverse problem is solved in the same way as the direct problem. The results

[*]Corresponding Author. E-mail: tmpm@tu.kielce.pl

confirmed that considerable heat transfer enhancement takes place at boiling incipience in the minichannel flow boiling. Moreover, under subcooling boiling, local heat coefficients exhibit relatively low values.

Keywords: Heat transfer; Incipience of flow boiling; Finite element method

Nomenclature

A	–	linear combination coefficient
$[A], [T], [V], [v]$	–	matrices
BI	–	boiling incipience
H	–	error functional
I	–	current supplied to the heating foil, A
J	–	number of elements
L	–	minichannel length, m
nn	–	number of nodes in an element
M, N	–	number of Trefftz functions used for approximation
P	–	number of measurement points
q_V	–	volumetric heat flux (capacity of internal heat source), W/m^3
S	–	cross-section, m^2
T	–	temperature, K
$\tilde{T}(x, y)$	–	temperature approximate, K
$u(x, y)$	–	particular solution of the nonhomogeneous equation
V	–	element of matrix, V
$v(x, y)$	–	Trefftz functions
x, y	–	spatial coordinates

Greek symbols

α	–	heat transfer coefficient, W/(m^{2}K)
δ	–	thickness, m
ΔU	–	voltage drop across the foil, V
$\varphi(x, y)$	–	base functions
λ	–	thermal conductivity, W/(mK)
Ω	–	plane domain

Subscripts

F	–	foil
G	–	glass
i, j, k, m, n	–	numbers
in	–	inlet
l	–	liquid
out	–	outlet
p	–	measurement point

1 Introduction

Miniature heat exchangers are used to provide higher cooling capacity for new technologies. This means a reduction in their size and cost but the identical power. Owing to the change of state, which accompanies flow boiling in minichannels, it is possible to meet contradictory demands simultaneously, i.e., to obtain a heat flux as large as possible at small temperature difference between the heating surface and the saturated liquid and, at the same time, retain small dimensions of heat transfer systems. Review of relevant literature and the selected publications covering heat transfer in minichannels is presented in [1–3].

Identification of heat transfer coefficient, presented in this article, belongs to the group of inverse heat conduction problems [4–6]. The inverse problem and the auxiliary direct problem were solved by means of the finite element method (FEM) in combination with the Trefftz method (FEMT). The idea of the Trefftz method was presented in [7] and consists in representing the approximate solution to the problem as a linear combination of functions which satisfy the governing equation strictly, while the set boundary conditions are satisfied approximately. Additional information on this method can be found in [8–12]. Combinations of Trefftz method and FEM was showed in [13–19].

2 Main goal

The objectives of the experimental investigations and calculations discussed in the present article focus on the evaluation of the heat transfer model and numerical approach to solving the inverse boundary problem, and the calculation of local heat transfer coefficient using the FEM with Trefftz functions. The application of liquid crystal thermography enables the determination of a two-dimensional temperature distribution on the heating surface.

3 Experimental set-up

The essential part is the test section with a vertical minichannel (Fig. 1a, 4) of 1.0 mm depth, 40 mm width and 360 mm length [3]. The heating element for the working fluid (R-123) flowing along the minichannel is an alloy foil (3) stretched between the front cover (6) and the channel body (7). It is possible to observe changes in the foil surface temperature through

the opening covered with glass (1). One side of the heating foil (between the foil and the glass) is covered with a base coat and liquid crystal paint (2). The test section body (7) contains channels which are either fed with water (5), or which are the air gaps. On the surface of the quasiadiabatic wall (7) constant temperature is maintained (the arithmetic mean of the temperatures at the inlet and outlet of the minichannel). In the inlet and the outlet of the minichannel pressure converters and thermocouples are installed.

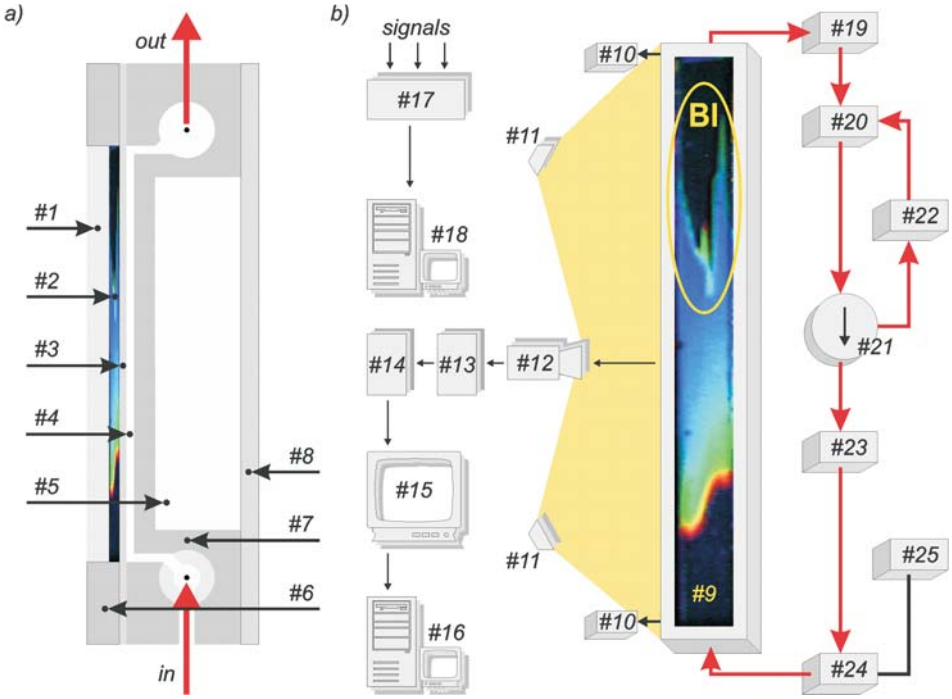

Figure 1. Diagrams of a) the test section: 1 – glass, 2 – liquid crystals, 3 – heating foil, 4 – minichannel, 5 – water channel, 6 – front cover, 7 – channel body (quasiadiabatic wall), 8 – rear cover, b) the main loop of the flow system and the data and color image acquisition system: 9-test section, 10 – pressure converter and thermocouple, 11 – lighting system, 12 – CCD video camera, 13 – RGB signal decomposer, 14 – Betacam recorder, 15 – monitor, 16 – computer with frame grabber and monitor, 17 – data acquisition station, 18 – computer with monitor, 19,22,24 – heat exchanger, 20 – compensating tank, 21 – rotary pump, 23 – rotameters, 25 – inverter.

In addition to the test section, the main loop consists is configuration of the following elements (Fig. 1b): 21 – rotary pump, 19, 22, 24 – heat exchangers

and 20 – compensating tank. The most important set-up elements for the flow, pressure and temperature control and measurement are the inverter (25), rotameters (23), pressure converters and thermocouples (10). The use of thermography has been made possible thanks to the color image acquisition system, Fig. 1b, which includes CCD video camera (12) with RGB signal decomposer (13), Betacam recorder (14) with monitor (15), and computer with frame grabber (16), monitor and specialist software. The registration of the remaining measurement data is carried out with (Keithley 500 A) data acquisition station (17), equipped with (ViewDac) software installed on another computer (18).

When the refrigerant flows along the minichannel, the increase in the electric power supplied to the heating foil causes boiling incipience in the minichannel. This is observed as a 'boiling front', which moves upstream together with the increase in applied heat flux [1–3]. The 'boiling front' is identified as a sudden drop in the temperature of the heating surface following its rise, at constant capacity of the internal heat source. Observation of the two-dimensional temperature distribution on the heating surface of the minichannel is possible owing to the liquid crystal thermography. A calibration procedure has to precede the virtual boiling heat transfer investigation. Its aim is to assign corresponding temperature values to the hues observed on the surface covered with liquid crystals.

4 Two-dimensional model

4.1 Problem formulation

In the two-dimensional approximation of heat transfer through major elements of the test section (Fig. 2), there occurs a direct problem in the glass barrier and an inverse problem in the heating foil [1,2]. To solve them, temperature measurements in the foil on the glass-side boundary, obtained thanks to the application of liquid crystal thermography, are used. When solving the inverse problem (no boundary condition on the boundary $y = \delta_G + \delta_F$), the temperature field and heat flux density in the foil on the boundary $y = \delta_G + \delta_F$ are determined. Local values of the heat transfer coefficient are calculated with the assumption of linear temperature distribution of the fluid flowing along the minichannel (measurement at minichannel inlet/outlet). It is assumed that in the foil operates a heat source of constant efficiency, distributed evenly in the entire volume of the foil. This volumetric heat flux supplied to the heating wall is determined

from the formula

$$q_V = \frac{I\Delta U}{S_F \delta_F} \,. \tag{1}$$

The temperature of the glass barrier, $T_G(x, y)$, satisfies the Laplace's equation

$$\nabla^2 T_G = 0 \,, \tag{2}$$

where $(x, y) \in \Omega_G = \left\{(x, y) \in \mathrm{R}^2 : 0 \le x \le L, \quad 0 \le y \le \delta_G\right\}$, and R^2 is the real plane.

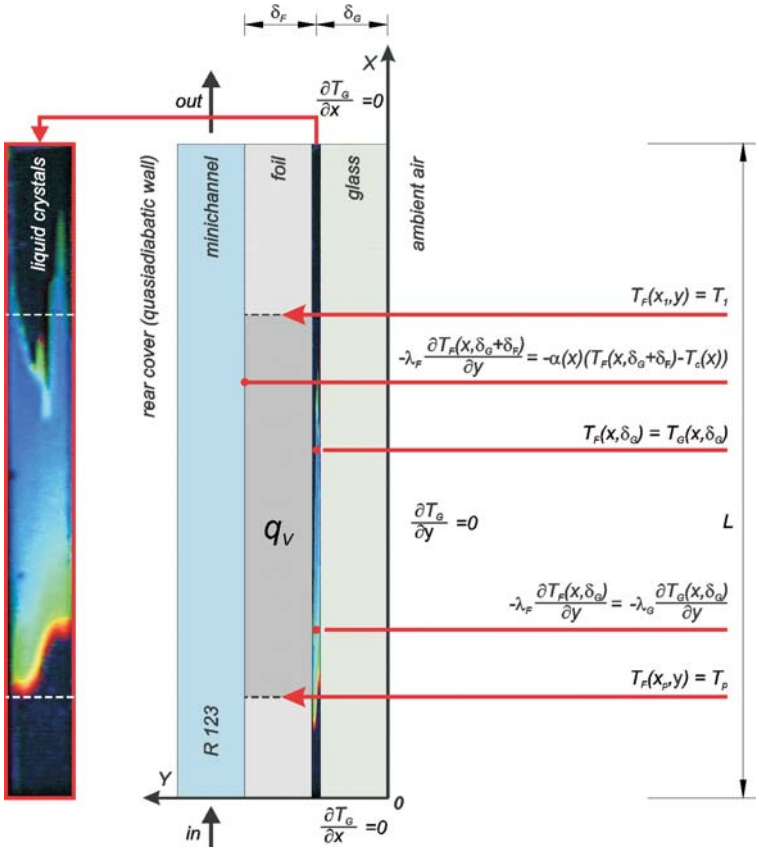

Figure 2. Boundary conditions for the two-dimensional approximation of heat transfer across main elements of the test section.

The temperature of the heating foil $T_F(x, y)$ satisfies the equation

$$\nabla^2 T_F = -\frac{q_V}{\lambda_F} \,, \tag{3}$$

where $(x,y) \in \Omega_F = \left\{(x,y) \in R^2 : x_1 \le x \le x_P, \quad \delta_G \le y \le \delta_G + \delta_F\right\}$, x_1 is the coordinate of the first temperature measurement point, and x_P is the coordinate of the final temperature measurement point.

For $y = \delta_G$ (the foil-glass boundary), the following conditions have been assumed:

$$T_F\left(x_p, \delta_G\right) = T_G\left(x_p, \delta_G\right) = T_p \quad \text{for} \quad p = 1, 2, \ldots P\,, \tag{4}$$

$$T_F\left(x, \delta_G\right) = T_G\left(x, \delta_G\right) \quad \text{for} \quad 0 \le x \le L\,, \tag{5}$$

$$-\lambda_F \frac{\partial T_F(x, \delta_G)}{\partial y} = -\lambda_G \frac{\partial T_G(x, \delta_G)}{\partial y} \quad \text{for} \quad 0 \le x \le L\,. \tag{6}$$

Conditions on other boundaries:

$$\frac{\partial T_G}{\partial y} = 0 \quad \text{for} \quad y = 0 \quad \text{and} \quad 0 \le x \le L\,, \tag{7}$$

$$\frac{\partial T_G}{\partial x} = 0 \quad \text{for} \quad x = 0 \quad \text{as well as} \quad x = L \quad \text{and} \quad 0 \le y \le \delta_G\,, \tag{8}$$

$$T_F(x_1, y) = T_1 \quad \text{for} \quad \delta_G \le y \le \delta_G + \delta_F\,, \tag{9}$$

$$T_F(x_P, y) = T_P \quad \text{for} \quad \delta_G \le y \le \delta_G + \delta_F\,. \tag{10}$$

The problem thus formulated was solved by means of the Trefftz functions (T-functions) [7–12]. These functions are used to solve both direct and inverse problems. The basic property of Trefftz functions is satisfying the governing equation. In the problem being discussed here, it is the Laplace's equation (2). What remains to be done is to adjust the linear combination of Trefftz functions to required initial and boundary conditions, and – in the case of inverse problems — also to the measurements, e.g., temperature.

In order to determine the value of heat transfer coefficient on the boundary, $y = \delta_G + \delta_F$, the temperature of the glass barrier, $T_G(x,y)$, is first determined from the solution of the direct problem, and subsequently the foil temperature, $T_F(x,y)$, is determined from the solution of the inverse problem. Knowing the foil temperature distribution enables the determination of local values of heat transfer coefficient on the heating foil–liquid boundary in the minichannel from the condition

$$-\lambda_F \frac{\partial T_F\left(x, \delta_G + \delta_F\right)}{\partial y} = \alpha\left(x\right)\left[T_F(x, \delta_G + \delta_F) - T_l\left(x\right)\right]\,, \tag{11}$$

where α is the sought heat transfer coefficient, and $T_l(x)$ is liquid temperature, approximated linearly along the entire minichannel length.

4.2 Finite element method with the use of T-functions

The solution method for Eqs. (2) and (3) is a generalisation of the method presented in [13]. In order to solve the formulated problem, domains Ω_G and Ω_F are divided into elements Ω_G^j and Ω_F^j. The approximate solution of Eq. (2) in each of the elements Ω_G^j is a linear combination of Trefftz functions

$$\tilde{T}_G^j(x,y) = \sum_{n=1}^{N} A_{jn} v_n(x,y) \ . \tag{12}$$

With the assumption that the temperatures $\tilde{T}_G^{jk}$ at the nodes (x_k, y_k) of the element Ω_G^j are known, coefficients A_{jn} are calculated from the linear systems of equations

$$\tilde{T}_G^j(x_k,y_k) = \tilde{T}_G^{jk} = \sum_{n=1}^{N} A_{jn} v_n(x_k,y_k), \quad k = 1,2,\ldots N \ . \tag{13}$$

In the abbreviated version, Eqs. (13) take the form $[v][A] = [T]$, whence upon inverting the matrix $[v]$, $[A] = [v]^{-1}[T] = [V]\ [T]$ is obtained. Therefore,

$$A_{jn} = \sum_{k=1}^{N} V_{nk} \tilde{T}_G^{jk} \ . \tag{14}$$

Substituting (14) into (12), the base functions for the element Ω_G^j are obtained in the following form:

$$\varphi_{jk}(x,y) = \sum_{n=1}^{N} V_{nk} v_n(x,y) \ . \tag{15}$$

These functions strictly satisfy Eq. (2) and have the following property:

$$\varphi_{jk}(x_{jm}, y_{jm}) = \begin{cases} 1 & \text{if} \quad k = m \\ 0 & \text{if} \quad k \neq m \end{cases} \ , \tag{16}$$

where (x_{jm}, y_{jm}) are the nodes of the element Ω_G^j. The temperature in each element Ω_G^j is a linear combination of base functions $\varphi_{jk}(x,y)$

$$\tilde{T}_G^j(x,y) = \sum_{k=1}^{nn} \varphi_{jk}(x,y)\ \tilde{T}_G^n \ , \tag{17}$$

where j is the number of the element in the domain Ω_G, k is the number of the node in the j-th element, n is the number of the node in the domain Ω_G, nn is the number of nodes in the j-th element.

The unknown coefficients $\tilde{T}_G^n$ of the linear combination (17) are determined by minimization of the functional H_G:

$$\begin{aligned} H_G = &\sum_{i=1}^{L2} \int_0^{\delta_G} \left[\frac{\partial \tilde{T}_G^{1+(i-1)L1}}{\partial x}(0,y)\right]^2 dy + \sum_{i=1}^{L2} \int_0^{\delta_G} \left[\frac{\partial \tilde{T}_G^{iL1}}{\partial x}(L,y)\right]^2 dy + \\ &+ \sum_{p_j=1}^{P} \left[\tilde{T}_G^j(x_{p_j},\delta_G) - T_{p_j}\right]^2 + \sum_{j=1}^{L1} \int_{x_{j-1}}^{x_j} \left[\frac{\partial \tilde{T}_G^j}{\partial y}(x,0)\right]^2 dx + \\ &+ \sum_{i=0}^{L2-1} \sum_{j=1}^{L1-1} \int_{y_i}^{y_{i+1}} \left[\tilde{T}_G^{j+iL1}(x_j,y) - \tilde{T}_G^{j+1+iL1}(x_j,y)\right]^2 dy + \\ &+ \sum_{i=0}^{L2-1} \sum_{j=1}^{L1-1} \int_{y_i}^{y_{i+1}} \left[\frac{\partial \tilde{T}_G^{j+iL1}}{\partial x}(x_j,y) - \frac{\partial \tilde{T}_G^{j+1+iL1}}{\partial x}(x_j,y)\right]^2 dy + \\ &+ \sum_{i=1}^{L2-1} \sum_{j=0}^{L1-1} \int_{x_j}^{x_{j+1}} \left[\tilde{T}_G^{(i-1)L1+j+1}(x,y_i) - \tilde{T}_G^{iL1+j+1}(x,y_i)\right]^2 dx + \\ &+ \sum_{i=1}^{L2-1} \sum_{j=0}^{L1-1} \int_{x_j}^{x_{j+1}} \left[\frac{\partial \tilde{T}_G^{(i-1)L1+j+1}}{\partial y}(x,y_i) - \frac{\partial \tilde{T}_G^{iL1+j+1}}{\partial y}(x,y_i)\right]^2 dx \ , \end{aligned} \tag{18}$$

where $L1$ is the number of elements in the Ox axis direction, $L2$ is the number of elements in the Oy axis direction.

In a similar way, foil temperature is determined. In each element Ω_F^j, it is presented in the form of a linear combination of base functions $\varphi_{jk}(x,y)$ defined by the Eq. (15)

$$\tilde{T}_F^j(x,y) = u(x,y) + \sum_{k=1}^{nn} \varphi_{jk}(x,y) \left[\tilde{T}_F^n - u(x_n,y_n)\right] \ , \tag{19}$$

where j is the number of the element in the domain Ω_F, n is the number of the node in the domain Ω_F, $u(x_n,y_n)$ is the value of the particular solution in the n-th node of the domain Ω_F, whereas k and nn carry the same meaning as in the Eq. (17). The unknown coefficients $\tilde{T}_F^n$ of the linear

combination (19) are determined by minimization of the functional H_F:

$$
\begin{aligned}
H_F = & \sum_{i=1}^{L4} \int_{\delta_G+\delta_F}^{\delta_F} \Big[\frac{\partial \tilde{T}_F^{1+(i-1)L3}}{\partial x}(x_1, y) - T_1\Big]^2 dy + \\
& + \sum_{i=1}^{L4} \int_{\delta_G+\delta_F}^{\delta_F} \Big[\frac{\partial \tilde{T}_F^{iL3}}{\partial x}(x_P, y) - T_P\Big]^2 dy + \\
& + \sum_{p_j=1}^{P} \big[\tilde{T}_F^j(x_{p_j}, \delta_G) - T_{p_j}\big]^2 + \sum_{j=1}^{L3} \int_{x_j}^{x_{j+1}} \big[\tilde{T}_F^j(x, \delta_G) - \tilde{T}_G^j(x, \delta_G)\big]^2 dx + \\
& + \sum_{j=1}^{L3} \int_{x_j}^{x_{j+1}} \Big[\lambda_F \frac{\partial \tilde{T}_F^j}{\partial y}(x, \delta_G) - \lambda_G \frac{\partial \tilde{T}_G^j}{\partial y}(x, \delta_G)\Big]^2 dx + \\
& + \sum_{i=0}^{L4-1} \sum_{j=1}^{L3-1} \int_{y_i}^{y_{i+1}} \big[\tilde{T}_F^{j+iL3}(x_j, y) - \tilde{T}_F^{j+1+iL3}(x_j, y)\big]^2 dy + \\
& + \sum_{i=0}^{L4-1} \sum_{j=1}^{L3-1} \int_{y_i}^{y_{i+1}} \Big[\frac{\partial \tilde{T}_F^{j+iL3}}{\partial x}(x_j, y) - \frac{\partial \tilde{T}_F^{j+1+iL3}}{\partial x}(x_j, y)\Big]^2 dy + \\
& + \sum_{i=1}^{L4-1} \sum_{j=0}^{L3-1} \int_{x_j}^{x_{j+1}} \big[\tilde{T}_F^{(i-1)L3+j+1}(x, y_i) - \tilde{T}_F^{iL3+j+1}(x, y_i)\big]^2 dx + \\
& + \sum_{i=1}^{L4-1} \sum_{j=0}^{L3-1} \int_{x_j}^{x_{j+1}} \Big[\frac{\partial \tilde{T}_F^{(i-1)L3+j+1}}{\partial y}(x, y_i) - \frac{\partial \tilde{T}_F^{iL3+j+1}}{\partial y}(x, y_i)\Big]^2 dx \ ,
\end{aligned}
\tag{20}
$$

where $L3$ is the number of elements in the Ox axis direction, $L4$ is the number of elements in the Oy axis direction.

5 Error analyses

5.1 The accuracy of heating foil temperature measurements by liquid crystal thermography and heat source efficiency measurement error

Evaluation of the accuracy of heating foil temperature measurements with liquid crystals thermography and heat source efficiency measurement error were discussed in [2]. Mean temperature measurement error of heating foil by liquid crystal thermography $\Delta T_F = 0.86$ K was obtained. The value of the relative heat source efficiency measurement amounted to 2.04%.

5.1.1 Measurement error of heat transfer coefficient

The mean relative error of heat transfer coefficients, similarly as in the work [1], was determined from the following formula:

$$\sigma_\alpha = \frac{\Delta\alpha}{\sum\limits_{k=1}^{P} \alpha(x_k)} , \tag{21}$$

where

$$\Delta\alpha = \left[\left(\sum_{k=1}^{P} \frac{\partial\alpha(x_k)}{\partial\lambda_F} \Delta\lambda_F \right)^2 + \left(\sum_{k=1}^{P} \frac{\partial\alpha(x_k)}{\partial T_F} \Delta T_F \right)^2 + \left(\sum_{k=1}^{P} \frac{\partial\alpha(x_k)}{\partial T_l} \Delta T_l \right)^2 + \left(\sum_{k=1}^{P} \frac{\partial\alpha(x_k)}{\partial \frac{\partial T_F}{\partial y}} \Delta \frac{\partial T_F}{\partial y} \right)^2 \right]^2 . \tag{22}$$

The heat transfer coefficient $\alpha = \alpha(\lambda_F, T_F, T_l, \frac{\partial T_F}{\partial y})$ is determined by formula (11), where $\Delta\lambda_F$ is the accuracy of the heat conductivity determination, $\Delta\lambda_F = 0.01$ W/(mK); ΔT_F is the accuracy of the foil temperature approximation (since the foil is very thin, we can assume that ΔT_F is equal to the error of the temperature measurement on the boundary $y = \delta_G$), $\Delta T_F(x_k, \delta_G) = 0.86$ K; ΔT_l is the liquid temperature measurement error, $\Delta T_l = 0.77$ K; $\Delta\frac{\partial T_F}{\partial y} = \left| \frac{1}{P} \sum\limits_{k=1}^{P} \frac{\partial^2 T_F(x_k)}{\partial y \partial x} \Delta x \right|$, here Δx denotes distance between the measuring points: $\Delta x = 7.388 \times 10^{-4}$ m. Table 1 presents examples of mean relative errors of the heat transfer coefficient. The mean relative error is in the range 3.06 to 3.41% and it tends to increase with the heating flux supplied to the heating area.

6 Experimental results

Boiling incipience is recognised as a sudden drop in the heating surface temperature that follows its systematic increase at constant capacity of the internal heat source. It is called 'boiling front' (BI) and it shifts in the direction opposite to the fluid flow in the minichannel with the increase in heat flux supplied to the heating surface [1–3]. Figure 3 shows examples of hue distribution on the foil surface, obtained with liquid crystal thermography, with a visible 'boiling front'.

Table 1. Mean relative errors of the heat transfer coefficient σ_α [%].

Set No. (see Fig. 4)	Mean relative error σ_α [%]
1	3.41
2	3.38
3	3.30
4	3.28
5	3.15
6	3.18
7	3.12
8	3.06

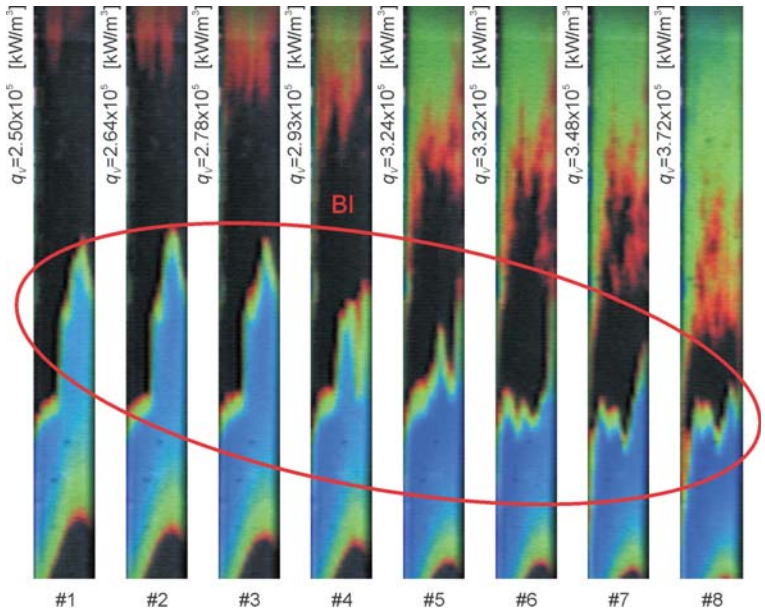

Figure 3. Images of temperature distribution on the heating wall, experimental data: flow velocity 0.35 m/s, mass flux 220 kg/(m^{2}s), pressure at the channel inlet 340 kPa, $q_V = 2.5 \times 10^5 - 3.7 \times 10^5$ kW/m^3.

Applied finite element method in combination with Trefftz method (FEMT) has used four T-functions: 1, x, y, xy. In the domains Ω_G and Ω_F, a rectangular mesh, parallel to the coordinate system axis, has been introduced. The domain Ω_G has been divided into 2 849 elements, and Ω_F into 651–1169 elements. In the domain Ω_G 3264 nodes have been placed, and in the domain Ω_F from 1304 to 2340 nodes. In each element Ω_G^j, Ω_F^j

a set of four nodes placed in the vertices of the rectangular element has been selected. The function $u(x, y) = -0.5 q_V \lambda_F^{-1} y^2$ has been assumed to be the particular solution of Eq. (3). Values of local heat transfer coefficients as a function of the distance from the inlet to the minichannel have been presented in Fig. 4. The dependence confirmed that considerable heat transfer enhancement takes place at boiling incipience un the minichannel flow boiling.

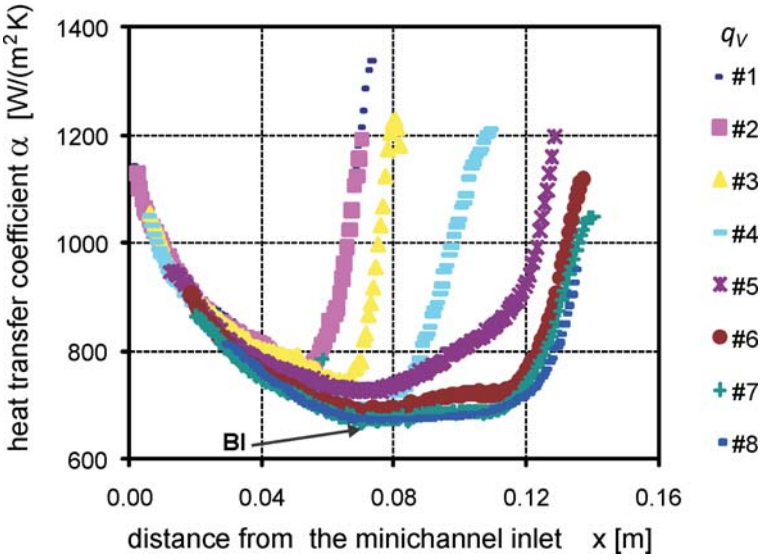

Figure 4. Heat transfer coefficient dependence on the distance along the minichannel length, data as in Fig. 3.

7 Conclusions

The paper presents the procedure of determining of the heat transfer coefficient by solving the inverse problem in the heating foil and the ancillary direct problem in the glass barrier. The problem under study has been solved by means of the finite element method in combination with the Trefftz method. Lagrange interpolation with the Trefftz function has been used for the construction of base functions in the finite element method. This is an analytical and numerical approach and the inverse problem has been solved in the same way as the direct one. This method allows solving problems which lack the boundary condition or when the number of boundary

conditions is excessive. In issues lacking the boundary condition, information collected from the measurements at points close to the boundary is required. In the considered problem the temperature of the heating foil is derived from measurements at $y = \delta_G$ since no condition at $y = \delta_G + \delta_F$ is available. The determined approximates of the glass barrier and heating foil temperatures strictly satisfy the respective differential equations (2) and (3). In the FEMT, the condition (4) is strictly satisfied (element nodes are placed at measurement points), while the remaining boundary conditions are approximately satisfied.

In the minichannel flow boiling, considerable heat transfer enhancement takes place at boiling incipience. It is observed as a sharp increase in the heat transfer coefficient.

Acknowledgements The research has been financially supported by the Polish Ministry of Science and Higher Education, Grant No. N N512 354037 for the years 2009–2012.

Received 12 February 2011

References

[1] Piasecka M., Maciejewska B.: *The study of boiling heat transfer in vertically and horizontally oriented rectangular minichannels and the solution to the inverse heat transfer problem with the use of the Beck method and Trefftz functions*. Exp. Therm. Fluid Sci. **38**(2012), 19–32.

[2] Hozejowska S., Piasecka M., Poniewski M.E.: *Boiling heat transfer in vertical minichannels. Liquid crystal experiments and numerical investigations*. Int. J. Therm. Sci. **48**(2009), 1049–1059.

[3] Piasecka M.: *An investigation into the influence of different parameters on the onset of boiling in minichannels*. Arch. Thermodyn. **33**(2012), 67-90.

[4] Alifanow O.M.: *Inverse heat transfer problems*. Springer-Verlag, Berlin 1994.

[5] Kurpisz K., Nowak A.J.: *Inverse thermal problems*. Int. Series on Comput. Mech. Pub., Southampton, and Boston, 1995.

[6] Ozisik M.N., Orlande H.R.B.: *Inverse heat transfer: fundamentals and applications*. Taylor & Francis, New York 2000.

[7] Trefftz E.: *Ein Gegenstück zum Ritzschen Verfahren*. 2 Int. Kongress für Technische Mechanik, Zürich (1926), 131–137.

[8] Kita E.: *Trefftz method: an overview*. Adv. Eng. Softw. **24**(1995), 3–12.

[9] Zielinski A.P.: *On trial functions applied in the generalized Trefftz method*. Adv. Eng. Softw. **24**(1995), 147–155.

[10] Herrera I.: *Trefftz method: A general theory*. Numer. Meth Part. D. E. **16**(2000), 561–580.

[11] Ciałkowski M., Frąckowiak A.: *Heat functions and their application to solving of heat conduction and mechanics problems*. WPP, Poznań 2000 (in Polish).

[12] Cialkowski M.J., Frąckowiak A.: *Solution of a stationary 2D inverse heat conduction problem by Trefftz method*. J. Therm. Sci. **11**(2002), 148–162.

[13] Cialkowski M.J.: *New Type of basic functions of FEM in application to solution of inverse heat conduction problem*. J. Therm. Sci. **11**(2002), 163–171.

[14] Kompis V., Toma M., Zmindak M., Handrik M.: *Use of Trefftz functions in non-linear BEM/FEM*. Comput. Struct. **82**(2004), 2351–2360.

[15] Maciejewska B.: *Application of the modified method of finite elements for identification of temperature of a body heated with a moving heat source*. J. Theor. App. Mech. **42**(2004), 771–787.

[16] Cialkowski M.J., Frackowiak A., Grysa K.: *Solution of a stationary inverse heat conduction problem by means of Trefftz non-continuous method*. Int. J. Heat Mass Tran. **50**(2007), 2170–2181.

[17] Wang H., Qin Q.: *Hybrid FEM with fundamental solutions as trial functions forheat conduction simulation*. Acta Mech. Solida Sin. **22**(2009), 487–498.

[18] Grysa K., Leśniewska R.: *Different finite element approaches for inverse heat conduction problems*. Inverse Probl. Sci. Eng. **18**(2010), 3–17.

[19] Grysa K., Maciąg A.: *Solving direct and inverse thermoelasticity problems by means of Trefftz base functions for finite element method*. J. Therm. Stresses **34**(2011), 378–393.